

The importance of ligand–ligand interactions in determining molecular geometry: the ligand close packing model

E.A. Robinson, G.L. Heard, R.J. Gillespie*

Department of Chemistry, McMaster University, 1280 Main Street West, Hamilton, Ontario, Canada L8S 4M1

This paper is dedicated to Lawrence S. Bartell on the occasion of his 75th birthday

Received 22 December 1998; accepted 14 January 1999

Abstract

In 1960 Bartell proposed that interligand repulsions in some simple organic molecules of the types CX_3 and CX_4 , are much more important in determining molecular geometry than had previously been generally supposed. In recent work we have shown that this concept can be extended to analogous molecules of beryllium and boron where X is F, OH, or O. Assuming as Bartell did that each ligand can be approximately represented as a hard sphere we have shown that each ligand can be assigned a radius that decreases in the series BeX_n , BX_n , CX_n , as the ligand charge decreases with increasing electronegativity of the central atom. In this article we present results that further extend this work to other ligands, such as Cl, CH_3 and NH_2 and to other central atoms, in particular nitrogen and oxygen which, unlike Be, B and C, have lone pairs in their valence shells. Bartell's original suggestion has now been developed into a useful and widely applicable model that we call the ligand close packing (LCP) model. © 1999 Elsevier Science B.V. All rights reserved.

Keywords: Molecular structure; VSEPR theory; Ligand close packing model; Contributions of L.S. Bartell

1. Introduction

In 1960, Larry Bartell [1] reinvestigated the structure of iso-butylene by electron diffraction because of inconsistencies in earlier data. He found that the two expected peaks for the nonbonded $C\cdots C$ distances could not be resolved, the two distances having essentially the same value of 150 pm. Accordingly he could not determine the bond angles with a great accuracy and he gave a value of approximately 112° for the Me–C–Me angle. As the three outer carbon atoms therefore form an approximately equilateral triangle

he came to the insightful conclusion that this was not just a coincidence but shows that the three carbon atoms can be considered to be close packed around the central carbon atom (Fig. 1). He proposed therefore that the shortening of the C– CH_3 bond in isobutene which has a length of 150.5 pm compared to the length of the C–C bond in diamond and *n*-alkanes of 153–154 pm and the observed shortening of all carbon–carbon single bonds adjacent to multiple carbon–carbon bonds can be attributed to the decrease in the number of repulsive interactions from four in diamond and saturated hydrocarbons to three in alkenes and two in alkynes. He concluded that there is, therefore, no need to invoke changes in hybridization at the central carbon atom or other electronic effects such as hyperconjugation to account for the

* Corresponding author. Tel.: + 1-905-525-9140; fax: + 1-905-522-2509.

E-mail address: gillespi@mcmaster.ca (R.J. Gillespie)

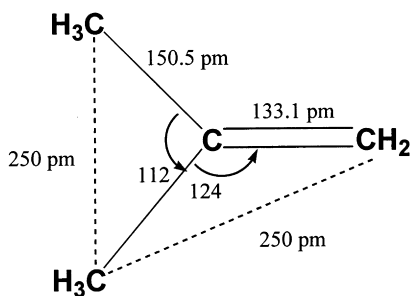


Fig. 1. Geometrical parameters for isobutene determined by Bartell and Bonham in 1960 [1].

observed variation of single bond lengths in hydrocarbons. Rather it is the closer packing of the ligands around the central carbon with decrease in coordination number that is mainly responsible for the bond shortening. Later a more accurate investigation based on both electron diffraction and microwave data [2] gave a value of 115.8° for the Me–C–Me angle and values of 255 and 249 pm for the $\text{H}_3\text{C}\cdots\text{CH}_3$ and $\text{H}_3\text{C}\cdots\text{CH}_2$ distances.

Subsequently, Bartell [3] went on to extend this idea to other ethenes, $\text{XX}'\text{C}=\text{CX}''\text{X}'''$, aldehydes and ketones, $\text{O}=\text{CXX}'$, and substituted methanes, where X = H, C, N, O, F, Cl, and Br, and showed that their geometries could similarly be explained solely on the basis of the close-packing of their X ligands. From the observed interligand distances he deduced a value for the interatomic nonbonded radius of each of these ligands, assuming that they could be regarded as ‘‘hard spheres’’. He also provided strong supporting evidence for the importance of nonbonded ligand interactions in molecules by showing that the vibrational spectra of the kind of molecule he was studying are better accounted for by a force field of the Urey–Bradley type which takes specific account of ligand–ligand interactions as well as bond stretching than by other types of force field which do not make a specific allowance for ligand–ligand interactions [4–8].

In 1985, Hargittai [9] published an extensive review of the geometry of a large number of molecules of the type XYSO_2 based on his own earlier work [10,11] and that of many others. In this review, he drew attention to the remarkably constant interligand distances in a large number of molecules. For example, he found that the $\text{O}\cdots\text{O}$ distances were all in

the range of 247–250 pm with an average value of 248 pm and nearly constant values of 238 pm for $\text{O}\cdots\text{F}$ distances and 279 pm for $\text{O}\cdots\text{Cl}$ distances. He concluded that interligand repulsions must be important in these molecules but because he found that these interligand distances are larger than the distances predicted by the sum of the Bartell radii he also concluded that they could not be the only factor determining the geometry of these molecules.

Glidewell [12,13] later extended Bartell’s table of radii to other atoms primarily on the basis of interligand distances in molecules of the type OX_2 and NX_3 . However, for ligands such as SiH_3 from which Glidewell deduced a ligand radius for Si there is good reason to believe that the ligands are not close packed [14]. The intramolecular radii deduced by Bartell and Glidewell are usually referred to as 1,3 radii or one angle radii. They have values that are intermediate between the commonly accepted values of covalent and van der Waals (or ionic) radii. However, the idea that interligand repulsive interactions play a major role in determining molecular geometry has not been generally accepted, probably because the radii deduced by Glidewell are not as reliable as those given by Bartell and, more importantly, as we will show, because the Bartell radii are only valid for ligands bound to carbon and are inappropriate for ligands bonded to other atoms.

In 1989 Baird [15] also came to the conclusion that bond angles in AX_2E_2 and AX_3E molecules are determined by the steric size of the ligand. He arrived at this conclusion on the basis of ab initio calculations at the 6-31G* level in which he studied how the bond angles in H_2O , F_2O , $(\text{CH}_3)_2\text{O}$ and Cl_2O varied with the XO bond length. He found that in the region of the equilibrium bond length the bond angle increased very rapidly with decreasing bond length indicating that to a reasonable approximation the ligands could be regarded as ‘‘hard spheres’’ and that it is the contact between these spheres at the equilibrium bond distance that determines the observed bond angle.

In this article we review some of the extensive evidence for the importance of ligand–ligand repulsive interactions in determining molecular geometry and show why this has not been generally recognized despite Bartell’s earlier convincing evidence from analysis of the structures of some simple organic

Table 1
Bond lengths, bond angles, and F...F distances in some molecules containing BeF_n, BF_n or CF_n groups^a

	Coordination number	A–F (pm)	∠FAF (°)	F...F (pm)
BeF ₃ ⁻	3	149	120.0	258
BeF ₄ ⁻	4	155.4	109.5	254
				Average: 256
F ₃ B	3	130.7	120.0	226
F ₂ B–OH		132.3	118.0	227
F ₂ B–NH ₂		132.5	117.9	227
F ₂ B–CH ₃		131.5	116.8	224
F ₂ B–Cl		131.5	118.1	226
F ₂ B–H		131.1	118.3	225
F ₄ B ⁻	4	138.2	109.5	226
F ₃ B–CH ₃ ⁻		142.4	105.4	227
F ₃ B–CF ₃ ⁻		139.1	109.9	228
F ₃ B–PH ₃		137.2	112.1	228
				Average: 226
CF ₃ ^{+b}	3	124.4	120.0	216
F ₂ C=CF ₂		131.9	112.4	219
F ₂ C=CCl ₂		131.5	112.1	218
F ₂ C=CH ₂		132.4	109.4	216
F ₂ C=CHF		133.6	109.2	218
F ₄ C	4	131.9	109.5	215
F ₃ C–CF ₃		132.6	109.8	217
F ₃ C–BF ₃ ⁻		134.3	104.9	213
F ₃ C–OF		131.9	109.4	215
F ₃ CO ⁻		139.2	101.3	215
				Average: 216

^a For more extensive data and references see Ref. [16].

^b Calculated structure.

molecules and Baird's theoretical work. And we show how the ligand close packing (LCP) model provides very simple explanations of the bond lengths and angles in some molecules that in the past have not been satisfactorily explained.

2. Bond lengths and bond angles in molecules of beryllium, boron, and carbon

Tables 1–4 summarize the geometric data for a selection of three- and four-coordinated molecules of beryllium, boron, and carbon where the ligands X are F, Cl, O, and C [16–18]. It can be seen that in all cases the close contact ligand–ligand distances are remarkably constant independent of coordination number and the presence of other ligands, providing good evidence for the importance of nonbonded ligand–ligand repulsions.

By taking one-half the interligand contact distances we have deduced a set of radii analogous to those given by Bartell but which we call *intramolecular ligand radii* or simply *ligand radii*. Values for the radii of the ligands discussed in this article are given in Table 5, where it can be seen that the radii of the ligands bonded to carbon agree well with Bartell's values but also that they vary depending on the atoms to which the ligand is bonded, decreasing from beryllium to boron to carbon. A more extensive set of radii based on other data not all of which has yet been published is given in Table 6. Some of these are preliminary values which may not be as reliable as the values in Table 5 but they illustrate how the radius of any given ligand varies with the atom to which it is bonded in every case decreasing from left the right across the periodic table. It has not been previously appreciated that the Bartell radii are not generally applicable but apply only to ligands bonded to carbon,

Table 2

Bond lengths, bond angles, and Cl···Cl distances in some molecules containing BeCl_n, BCl_n, or CCl_n groups^a

	Coordination number	A–Cl (pm)	∠ClACl (°)	Cl···Cl (pm)	
Cl ₂ Be(NCMe) ₂	4	197.8	116.8	337	
Cl ₂ Be(Oet ₂) ₂		197.8	116.6	337	
				Average: 337	
BCl ₃	3	174.2	120.0	301	
Cl ₂ B–BCl ₂		175.0	118.7	301	
Cl ₂ BB ₅ H ₈		172.0	127.7	300	
[Cl ₂ B(NPPh ₃) ₂]	4	188.4	105.4	300	
BCl ₄ [−]		183.3	109.5	299	
H ₃ N–BCl ₃		183.8	111.2	303	
C ₅ H ₅ N–BCl ₃		183.7	110.1	301	
Me ₃ N–BCl ₃		183.1	109.3	299	
Me ₃ P–BCl ₃		185.5	110.9	306	
Ph ₃ P–BCl ₃		185.1	109.5	302	
				Average: 302	
CCl ₃ ^{+b}		3	166.3	120.0	258
Cl ₂ CO			173.8	111.8	288
Cl ₂ C=CH ₂	171.8		112.4	286	
Cl ₂ C=CF ₂	4	170.6	119.0	294	
CCl ₄		177.1	109.5	289	
H ₂ CCl ₂		176.5	112.0	293	
F ₂ CCl ₂		174.4	112.5	290	
Me ₂ CCl ₂		179.9	108.3	292	
Cl ₃ C–CCl ₃		176.9	108.9	288	
Cl ₃ CH		175.8	111.3	290	
Cl ₃ CF		176	109.7	291	
				Average: 287	

^a For more extensive data and references see Ref. [20].^b Calculated structure.

so it is clear why the Bartell radii were found not to account for interligand distances in molecules with a central atom other than carbon. This is doubtless the main reason why Bartell's ideas were not generally accepted and why in assessing the importance of steric factors most chemists have continued to rely on comparisons with ligand–ligand distances calculated from van der Waals radii. But why does the size of a ligand depend on the atom to which it is bonded? As we will see the size of a ligand depends on its charge and the charge depends very much on the atom to which it is bonded.

3. Atomic charges

The charges on atoms in molecules can be obtained using the AIM (Atoms in Molecules) theory [19] to analyse the molecular electron density distribution

calculated by ab initio methods. Tables 7–9 give values of atomic charges calculated by this method for the fluorides, chlorides, and hydroxides of the elements in Period 2 [16–18,20]. We illustrate the use of the AIM analysis of the electron density distribution by the contour diagram of the electron density of the BF₃ molecule in Fig. 2. Each nucleus is surrounded by a region of high electron density which decreases rapidly with increasing distance from the nucleus. Between each pair of bonded nuclei there is a line along which the electron density is greater than in the surrounding region, in other words a line along which the electron density is concentrated. This line is called a *bond path*. Along this line is a point at which the electron density reaches a minimum value. This point is called the *bond critical point*. Passing through this point is a line that follows the valley of minimum density in the two-dimensional contour map between two nuclei

Table 3

Examples of average bond lengths, bond angles, and O···O distances in some molecules containing BeO_n, BO_n, and CO_n groups^a

	Coordination number	A–O (pm)	∠OAO (°)	O···O (pm)
Y ₂ BeO ₄	3	154.3	120	267
SrBe ₃ O ₄		154.3	120.0	266
BeO(s)	4	164	109.5	268
Li ₁₄ Be ₃ B(BO ₃) ₉		162	109.4	265
SrBe ₃ O ₄		164	109.5	268
LiBePO ₄ ·H ₂ O		163	109.5	266
				Average: 266
[HBO] ₃	3	137.6	120.0	238
[EtBO] ₃		138.4	118.4	238
[PhBO] ₃		138.6	118.0	238
Ag ₃ BO ₃		137.8	120.0	238
FeBO ₃		137.9	120.0	238
K ₃ B ₃ O ₆		1 133.0	1–2 121.3	238
		2 139.8	2–2 117.3	239
				Average: 238
NH ₄ ⁺ HCO ₂ ⁻	3	1 123.7	126.3	222
		2 124.6		
Li ⁺ CH ₃ CO ₂ ·2H ₂ O		124.5	125.7	222
Ca ²⁺ (ClCH ₂ CO ₂ ⁻) ₂		125.4	126.4	222
Na ⁺ HCO ₃ ⁻		126.4	125.0	222
Ca ²⁺ CO ₃ ⁻		128.2	120.0	222
				Average: 222

^a For more extensive tables, including complex borates, and references see Ref. [17].

Table 4

Examples of average bond lengths, bond angles, and C···C distances in some molecules containing BC_n, and CC_n groups^a

	Coordination number	Bond length (pm)	Bond angle (°)	C···C (pm)
B(CH ₃) ₃	3	157.8	120.0	273
(CH ₃) ₂ B[N(H)CH ₃]		158.6	119.8	274
(CH ₃) ₂ BN ₃		156.9	115.1	265
(CH ₃) ₂ BNCO		156.3	123.6	276
(C ₆ H ₅) ₂ BCl		155.9	123.3	274
B(CH ₂ CH ₃) ₃		157.3	120.0	273
B(C ₆ H ₅) ₃		158	120.0	274
Na ⁺ HB(CH ₃) ₃ ⁻	4	164	111	270
				Average: 272
(H ₃ C) ₂ C=C(CH ₃) ₂	3	1 150.5	1–1 113.2	251
		2 133.6	1–2 123.4	250
(H ₃ C) ₂ C=CH ₂		1 150.7	1–1 115.8	255
		2 134.2	1–2 122.1	249
<i>trans</i> -(CH ₃)HC=CH(CH ₃)		1 150.9	1–2 123.8	252
		2 134.8		
C ₃ H ₈ ·C ₇ H ₁₆	4	153.1–153.9	111.9–112.9	254–255
(CH ₃) ₂ CHCl		152.7	112.7	254
(HCCl ₂) ₂ CH ₂		152.7	114.2	256
(H ₂ CCl) ₂ CH ₂		153.1	111.6	253
(BrCH ₂) ₂ CH ₂		152.7	111.4	252
Diamond		154.4	109.5	252
				Average: 253

^a For more extensive data and references see Ref. [20].

Table 5
Ligand radii (pm) for the molecules discussed in this article

Ligand	Anion ^a	Central atom			Bartell
		Be	B	C	
C			137	126	125
O	126 (140)	134	120	113	114
F	119 (136)	128	113	108	108
Cl	167 (181)	168	151	144	144
		Si	P	S	
O	126 (140)	132	127	124	114
F	119 (136)	127	118	114	108
Cl	167 (181)	164	156	154	144

^a For the anion radii see Ref. [17]. The anion values in parentheses are from L. Pauling, *The Nature of the Chemical Bond*, 3rd Ed., Cornell University Press, Ithaca, 1960.

that are connected by a bond path. This line is the intersection of the *interatomic surface* between the two atoms with the plane of the molecule in the three-dimensional electron density distribution. From the method used to define this surface it is also called a *zero-flux surface*. These interatomic surfaces are the only unambiguous and quantum mechanically sound way to partition a molecule into its component atoms. Any properties of an atom calculated on the basis of this definition of the atom are accurately additive to give the value of the particular property for a group of atoms or the complete molecule. The *charge* on an atom is, for example, obtained by integrating the electron density of the atom as defined by its interatomic surfaces and then subtracting the nuclear charge. The *electron density at the bond critical point* is given the symbol ρ_b . Values of ρ_b are given in Tables 7–9. The electron density at the bond critical point, ρ_b , is an approximate measure

Table 6
Ligand radii (pm): A more extensive set

Central atom	Be	B	C	N	O	Si	P	S
C		137	125	120	117			
N	144	124	119			144	135	
O	133	119	114			132	127	124
F	128	113	108	108		127	118	114
Cl	168	151	144	142	140	164	156	154
H		110	90	82	76	120	103	97

of the amount of electron density accumulated between the nuclei and therefore of the covalent character of the bond.

We see that for the fluorides the charge on the ligand decreases from a very large value approaching the -1 charge of the F^- ion to zero in F_2 following closely the decrease in the difference in the electronegativities of the central atom and the ligand. When the ligand charge approaches the full ionic charge the ligand radius is comparable to that of the corresponding anion. As the charge decreases from this value across the period the ligand radius decreases correspondingly. As a result of the magnitude of the charge on the ligand the charge on the central atom increases from Li to C to a maximum of $+2.43$ for BF_3 and to the essentially identical value of $+2.45$ for CF_4 and then decreases rapidly. The electrostatic attraction between these large charges contributes greatly to the strength of the bonds decreasing their length considerably from LiF to BF_3 and making the BF bond the strongest known single bond with an average bond energy of 632 kJ mol^{-1} . As the AF bond length decreases the electron density between the nuclei increases rapidly as can be seen from the ρ_b values in Table 7 reaching a maximum value of 0.314 e au^{-3} for NF_3 and then decreasing only very slightly in these predominately covalent molecules. The rather large ρ_b values together with the large atomic charges for BF_3 and CF_4 indicate that the bonds can be regarded as both strongly ionic and strongly covalent.

The charges in the hydroxides (Table 8) are slightly smaller than in the fluorides and follow a similar pattern with the OH group becoming slightly positive in FOH. The charges in the chlorides (Table 9) are considerably smaller than in the fluorides consistent with the smaller electronegativity of chlorine. Consequently the chlorine has a positive charge in NCl_3 , OCl_2 , and FCl and, whereas the CF_4 molecule has a considerable ionic character while at the same time being rather strongly covalent, the CCl_4 molecule is predominately covalent.

4. The ligand close packing model

We call the model proposed by Bartell from a consideration of interligand distances in organic

Table 7
AIM atomic charges and ρ_b values for the Period 2 molecular fluorides^a

	Bond length (pm)	Bond angle (°)	ρ_b (au) ^b	$-q(\text{F})$	$q(\text{A})$
LiF	157.3 (156.4)		0.075	0.92	0.92
BeF ₂	137.8 (140)	180 (180)	0.145	0.88	1.75
BeF ₃ ⁻	147.6 (149)	120 (120)	0.104	0.91	1.75
BeF ₄ ²⁻	160.0 (155.4)	109.5 (109.5)	0.070	0.94	1.76
BF ₃	131.4 (130.7)	120 (120)	0.217	0.81	2.43
BF ₄ ⁻	141.1 (138.6)	109.5 (109.5)	0.164	0.86	2.43
CF ₃ ⁺	123.5	120 (120)	0.373	0.53	2.59
CF ₄	132.6 (131.9)	109.5 (109.5)	0.309	0.61	2.45
NF ₃	138.2 (138.5)	101.9 (102.3)	0.314	0.28	0.83
NF ₄ ⁺	131.8 (130)	109.5 (109.5)	0.387	0.08	1.32
OF ₂	140.4 (140.5)	104.0 (103.1)	0.295	0.13	0.27
F ₂	139.9 (141.8)		0.288	0	0

^a Experimental data are given in parentheses.

^b 1 au = 1 e a₀⁻³ = 1 e bohr⁻³.

molecules, and extended by us to many other molecules, the Ligand Close Packing (LCP) model. We arrived at this model by an independent route from Bartell and only then remembered his work that had been published nearly thirty years previously. We were studying the bonding and geometry of fluorides and realized that the constancy of the interligand distances and their correlation with the ligand charges suggested that these molecules can be considered to consist of anion-like ligands packed around a cation-like central atom much as anions are packed around cations in a crystalline solid. However, it is clear from Bartell's work and our own that even ligands with only very small charges can be considered to be close packed around a central atom and that this is an important factor in determining their molecular geometry.

The ligand radii in Tables 5 and 6 were obtained

Table 8
Calculated bond lengths, bond angles, atomic charges and ρ_b values for the Period 2 molecular hydroxides

	A–X (pm)	XAX (°)	$q(\text{OH})$	$q(\text{A})$	ρ_b (au)
LiOH	158.2	—	– 0.91	– 0.91	0.073
Be(OH) ₂	142.3	180	– 0.85	1.70	0.133
B(OH) ₃	136.9	120	– 0.76	+ 2.28	0.204
C(OH) ₄	139.3	103.6, 112.5	– 0.50	+ 1.99	0.289
N(OH) ₃	139.9	103.8	– 0.13	+ 0.40	0.311
O(OH) ₂	144.4	100.3	+ 0.04	– 0.08	0.281
FOH	143.2	—	+ 0.19	– 0.19	0.269

from the distances between two ligands of the same kind but they should also apply to molecules with different kinds of ligands. The distances between two different ligands should be given by the sum of the appropriate ligand radii. That this is the case is shown but the data in Tables 10–14 which compare O···F, O···Cl, Cl···F, C···F and C···Cl interligand distances with the values predicted from the sum of the ligand radii [12–15,17]. The good agreement between the observed and predicted interligand distances provides further strong evidence for the validity of the LCP model at least for molecules in which Be, B or C are the central atom.

In the following sections we discuss:

Table 9
AIM atomic charges and ρ_b values for the Period 2 molecular chlorides

	Bond length (pm) ^a	$q(\text{Cl})$	$q(\text{A})$	ρ_b
HCl	128.4 (127.5)	– 0.25	+ 0.25	0.240
LiCl	202.2 (220.1)	– 0.91	+ 0.91	0.047
BeCl ₂	179.8	– 0.84	+ 1.68	0.097
BCl ₃	174.9 (174.2)	– 0.64	+ 1.93	0.157
CCl ₄	179.7 (177.1)	– 0.09	+ 0.35	0.182
CCl ₃ ⁺	165.8	+ 0.22	+ 0.33	0.235
NCl ₃	179.1 (175.9)	+ 0.08	– 0.24	0.176
OCl ₂	172.8 (170)	+ 0.23	– 0.46	0.184
FOCl	166.4 (162.8)	+ 0.38	– 0.38	0.187

^a Experimental data are in parentheses.

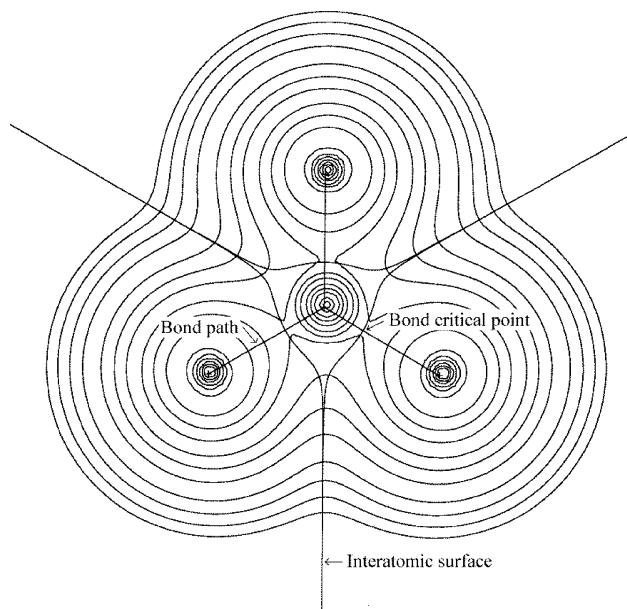


Fig. 2. Electron density contour map for the plane of the BF_3 molecule. Values of the contours are $\rho(r) = 0.001, 0.002, 0.004, 0.008, 0.02, 0.04, 0.08, 0.2, 0.4, 0.8, 2.0, 4.0, 8.0, 20.0, 40.0, 80.0$ au ($1 \text{ au} = 1 \text{ e bohr}^{-3}$).

Table 10

Experimental and predicted $\text{O}\cdots\text{F}$ interligand distances in some oxofluoroboron and oxofluorocarbon molecules

	Bond lengths (pm)		$\angle\text{FAO}$ ($^\circ$)	$\text{O}\cdots\text{F}$ (pm) ^a
	B–F or C–F	B–O or C–O		
$\text{F}_3\text{B–OH}_2$	138.2	153.2	105.9	233
	138.3		106.5	234
$\text{F}_3\text{B–O(H)Me}$	139.9	152.4	105.7	233
	135.5		106.0	230
$\text{F}_2\text{B–OH}$	132.3	134.4	122.8	234
$\text{F}_2\text{B–O}^-$	140.5	120.7	126.8	234
				Average: 233
$(\text{CF}_3)_2\text{O}$	132.7	136.9	110.2	221
CF_3O^-	139.2	122.7	116.2	223
CF_3OF	131.9	139.5	109.6	222
F_2CO	131.7	117.0	126.2	222
F(Me)CO	134.8	118.1	121.7	221
F(Cl)CO	133.4	117.3	123.7	221
F(Br)CO	131.7	117.1	125.7	222
<i>trans</i> - FC(O)OF	132.4	117.0	126.5	223
<i>cis</i> - FC(O)OF	132.0	117.2	126.4	223
FC(O)NO_3	132.0	116.5	128.8	224
$[\text{FC(O)}]_2$	132.9	118.0	124.2	222
				Average: 222

^a Predicted $\text{O}\cdots\text{F}$ distance: B = 232 pm, C = 223 pm.

Table 11
Experimental and predicted O...Cl interligand distances in some oxochlorocarbon molecules

	Bond lengths (pm)		$\angle \text{ClCO} (^{\circ})$	O...Cl (pm) ^a
	C–Cl	C–O		
Cl ₂ CO	173.8	117.6	124.1	259
Cl(F)CO	172.5	117.3	127.5	261
Cl(Br)CO	173.8	117.3	123.5	258
[ClC(O)] ₂	174.6	118.3	124.1	260
MeC(O)Cl	179.6	118.5	121.2	261
				Average: 260

^a Predicted O...Cl distance: 261 pm.

1. the use of the model to provide an understanding of the geometry of BF₃ and related molecules, and OCF₃⁻ and ONF₃,
2. the extension of the model to molecules of nitrogen and oxygen in which the nitrogen or oxygen have lone pairs in their valence shells, and
3. molecules which have stereochemically inactive or weakly active lone pairs.

4.1. Bond lengths in three- and four-coordinated molecules of beryllium, boron, and carbon

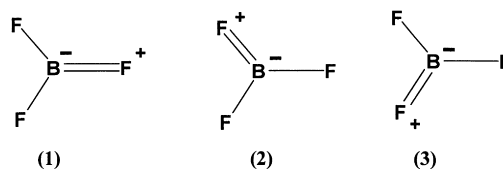
Three-coordinated molecules such as BF₃, BCl₃, and CF₃⁺ have much shorter bonds than the corresponding four-coordinated molecules such as BF₄⁻, BCl₄⁻, and CF₄. The lengths of the bonds in these molecules (Tables 1 and 2) are fully consistent with the ligand close packing (LCP) model. It is noteworthy that the ratio of the bond length in a four-coordinated molecule to that in the corresponding

Table 12
Experimental and predicted F...Cl interligand distances in some chlorofluorocarbon molecules

	Bond lengths (pm)		$\angle \text{FCCl} (^{\circ})$	F...Cl (pm) ^a
	C–F	C–Cl		
FCCL ₃	133	176	109.3	253
F ₂ CCl ₂	134.5	174.4	109.5	253
F ₃ CCl	132.8	175.1	110.4	254
F ₂ C(H)Cl	135.0	174.7	110.1	255
F(Cl)CO	133.4	172.5	108.8	250
				Average: 253

^a Predicted F...Cl distance: 253 pm.

three-coordinated molecule is close to the ratio of 1.06 for the packing of equivalent spheres around a central point even though this is a very approximate model for the molecules we are considering. Fig. 3 shows that the ligands cannot be described as true spheres but rather as having an approximately spherical shape with a flattened face in the bonding direction. The very short length of the BF bond in BF₃, for example, has commonly been attributed partly to the polarity of the bonds and to back-bonding in BF₃, giving the BF bonds some double bond character as described by the resonance structures (1) to (3)



but it is more simply accounted for by the small coordination number of boron as well as the polarity of the bonds without the need to postulate back-bonding [12,13]. In particular the LCP model gives a simple explanation for the large difference in the bond lengths BF₃ and BF₄⁻. Similar considerations apply to BCl₃ and BCl₄⁻ and to CF₃⁺ and CF₄.

4.2. The geometry of OCF₃⁻ and ONF₃

In many molecules there are two or more different ligands forming bonds of different lengths but they are still close packed, as the examples in Tables 10–14 show. When one of the ligands is bonded much more strongly than the others, the most strongly bonded ligand, in this case O, forms the shortest bond and the other bond lengths adjust to maintain the close-packing. For example, the CF bonds in CF₄ have a length 131.9 pm (Fig. 3) but when one of the F ligands is replaced by an O ligand to give the COF₃⁻ ion the CF bonds increase in length to 139.4 pm because the CO bond has a much shorter length of 122.7 pm than the CF bond that it replaces [21]. The O ligand pushes the neighboring fluorine ligands away increasing the CF bond lengths and decreasing the FCF angle from 109.5 to 101° until the interligand distances attain their usual values (Fig. 3). Removal of an F⁻ ion to give COF₂ which is only three- rather than four-coordinated decreases the CO bond length to 117.0 pm and the CF bond length to 131.7 pm while the O...F and

Table 13

Experimental and predicted C...Cl interligand distances in some chlorocarbon molecules

	Bond lengths (pm)		\angle CCCl ($^\circ$)	C...Cl (pm) ^a
	C–C	C–Cl		
(CH ₃) ₂ CCl ₂	152.3	179.9	108.9	271
CH ₃ CH ₂ Cl	152.8	174.6	110.7	274
CH ₃ C(O)Cl	150.8	179.8	112.2	275
[C(O)Cl] ₂	153.6	174.6	111.7	272
[(H ₃ C) ₃ C] ₃ CCl	182.8	152.8	117.3	271
Cl ₂ C=CCl ₂	135.5	171.9	122.2	270
Cl ₂ C=CF ₂	131.5	170.6	120.5	266
H ₂ C=C(H)Cl	135.5	172.8	121.1	269
Cl ₂ C=C=CH ₂	132.6	173.3	122.2	269
				Average: 271

^a Predicted C...Cl distance: 271 pm.

F...F distances retain their normal values of 215 and 222 pm, respectively (Fig. 3) [22]. The unexpectedly long CF bonds in OCF₃⁻ have been the subject of much discussion which is usually based on the octet rule and the use of the resonance structures to describe the bonding. As the CO bond has a length comparable to that in H₂CO (120.9 pm) and F₂CO (117.0 pm) and much shorter than the CO bond in CF₃OH which has a calculated length of 132.8 pm [22] it is usually represented as double bond as in (4) but here the carbon atom appears to be pentavalent thus violating the octet rule. To avoid this problem resonance structures such as (5) to (8) are usually written. However, while

structure (5) obeys the octet rule it is given little weight because it appears to imply a relatively long CO single bond.

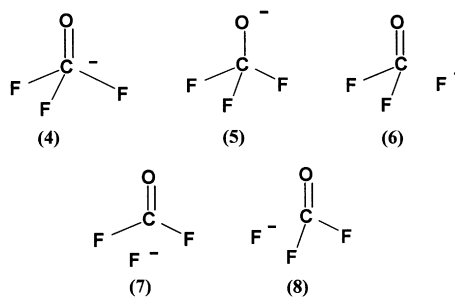


Table 14

Experimental and predicted C...F interligand distances in some fluorocarbon molecules

	Bond distance (pm)		\angle CCF ($^\circ$)	C...F (pm) ^a
	C–F	C–C		
F ₃ C–CF ₃	132.6	154.5	109.8	235
[(F ₃ C) ₃ C] ₃ COH	133.5	156.6	110.6	239
(F ₃ C) ₃ –CH	133.6	153.9	110.9	237
(F ₃ C) ₃ –CF	142.9	152.4	107.9	239
(F ₃ C) ₃ –Cl	133.3	154.4	111.0	327
H ₃ CC(O)F	136.2	150.5	110.5	236
F ₂ C=CF ₂	131.9	131.1	123.8	232
F ₂ C=CCl ₂	131.5	134.5	124.0	235
F ₂ C=CH ₂	131.6	132.4	125.2	234
<i>cis</i> -F(H)C=CF(H)	133.5	133.1	124.7	235
<i>trans</i> -F(H)C=CF(H)	134.4	132.9	119.3	231
F(H)C=CH ₂	134.8	133.3	121.0	233
				Average: 235

^a Predicted C...F distance: 234 pm.

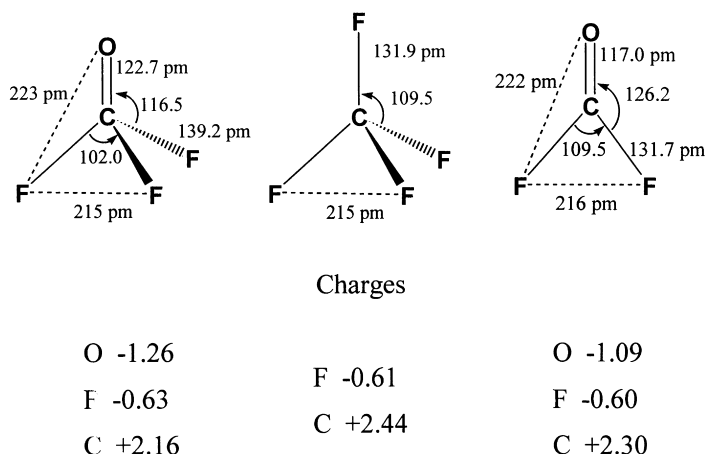


Fig. 3. Geometrical parameters and atomic charges for OCF_3^- , CF_4 and OCF_2 .

Consequently the CF single-bond–no-bond resonance structures were introduced to give a description of the bonding that is consistent with the length of the CF bonds. However, these resonance structures are merely a description of the bonding in terms of the Lewis model but does not *explain* the geometry. Moreover, they predict an incorrect distribution of charge with all the negative charge distributed among the fluorine ligands rather than on oxygen whereas the charge on O in COF_3^- (1.26) is twice that of F (0.63). The large charge on oxygen is an important reason why it is bonded so strongly to the carbon and forms a very short bond.

The bond lengths and angles in ONF_3 (Fig. 4) which is isoelectronic with OCF_3^- have a similar pattern to those in OCF_3^- and their interpretation has caused similar controversial discussion. The NO bond has a length of 115.8 pm which is comparable to that in NO_2^+ (115 pm) in which the bonds are considered to be double bonds, while the NF bonds with a length of 143.1 pm are considerably longer than those in NF_4^+ (130 pm). The Lewis

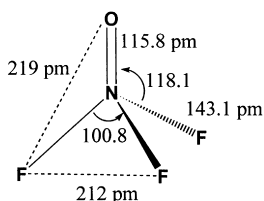
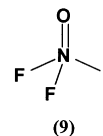


Fig. 4. Geometrical parameters for ONF_3 .

structure (9)



implies a pentavalent nitrogen that similarly appears to contravene the octet rule and does not explain the very long NF bonds. The geometry of this molecule can be explained by the LCP model in just the same way as for OCF_3^- . The F ligands are pushed away from the nitrogen by the strongly bonded O ligand increasing the NF bond lengths and increasing the ONF angle to 118.1° .

The preceding discussion shows that the bonding in molecules such as OCF_3^- and ONF_3 cannot be adequately represented by Lewis structures. An important limitation of these structures is that they do not clearly show the polar character of the bonds and as a consequence structures such as (4) and (9) appear to contravene the octet rule whereas they do not if allowance is made for the polarity of the bonds. Moreover, the use of resonance structures to describe this polarity is based on a knowledge of the geometry and so such structures cannot be said to explain the geometry. In contrast the LCP model gives a clear explanation of the bond lengths and bond angles in these molecules. The molecules OCF_3^- and ONF_3 are examples of hypervalent molecules in that their conventional Lewis structure do not obey the octet rule.

Table 15
Bond lengths and bond angles in NX_3E molecules

	N–X (pm)	XNX (°)	X···X (pm)
NH_3	101.5	107.2	164
NF_3	136.5	102.3	212
NCl_3	175	106.8	280
$N(CH_3)_3$	145.8	110.9	240
$N(SiH)_3$	173.4	120	300

4.3. Ligand close packing and the VSEPR model

The VSEPR model is based on the assumption that interactions between nonbonding and bonding electron pairs in the valence shell of the central atom A in an AX_nE_m molecule are the dominant factor in determining geometry. In contrast the LCP model assumes that the interaction between the ligands is the major factor in determining geometry. For AX_n molecules in which the central atom has no lone pair electrons in its valence shell, the two models predict exactly the same geometries. It might appear that the LCP model would predict that a molecule such as NF_3 or NCl_3 would have a planar triangular geometry. However, this neglects the presence of the lone pairs which according to the VSEPR model take up space in the valence shell and which can be

regarded as pseudo ligands. The domains of lone pairs spread out to occupy as much of the valence shell as possible, denying this space to the ligands, and crowding the ligands together until they touch. In other words from the point of view of the LCP model a lone pair behaves like a special type of ligand that takes up as much space as possible. Thus the interligand radii in Tables 5 and 6 determine the bond angles in AX_3E and AX_2E_2 molecules as we will now see for some NX_3E and OX_2E_2 molecules.

Experimental data for some NX_3E molecules are given in Table 15. Only the molecules NH_3 , NF_3 , and NCl_3 have bond angles that are smaller than tetrahedral. In these molecules the ligands, except H, are more electronegative than N and so that the lone pair is well localized and behaves like a pseudo ligand crowding the ligands together so that the bond angles are smaller than 109.5° . Hydrogen as a ligand behaves as if it had a greater electronegativity than 2.2 which is close to the value for carbon (2.5) in that it localizes the valence shell electrons of NX_3 and OX_2 molecules more strongly than does carbon. This enhanced localizing effect of H as a ligand results from the much shorter length of an A–H bond than an A–C bond. Moreover, as a hydrogen ligand has no core or other nonbonding electrons, its electron density occupies relatively little space in the valence shell of the central atom and it forms correspondingly small bond angles.

Table 16
Bond lengths and bond angles in NX_2YE and NXY_2E molecules

	Bond	Bond length (pm)	Bond angle	Bond angles (°)	X···X	Observed (pm)	Predicted (pm)
NH_2CH_3	N–H	101.1	HNH	105.9	H···H	161	164
	N–C	147.4	HNC	112.1	H···C	208	202
$NH(CH_3)_2$	N–H	102.2	HNC	108.8	H···H	204	202
	N–C	146.6	CNC	111.6	C···C	243	240
NHF_2	N–H	102.9	HNF	101.6	H···H	161	164
	N–F	140.0	HNF	99.8	H···F	191	189
$NF(CH_3)_2$	N–F	144.7	CNC	112.0	C···C	242	240
	N–C	146.2	FNC	104.6	F···C	229	227
$NF_2(CH_3)$	N–F	141.3	FNF	101.0	F···F	218	214
	N–C	144.9	FNC	103.6	F···C	229	227
NF_2Cl	N–F	138.2	FNF	103	F···F	216	214
	N–Cl	173.0	FNCI	105	F···Cl	248	249
$NCl_2(CH_3)$	N–Cl	174	CINCl	108	Cl···Cl	282	283
	N–C	142	CINC	109	Cl···C	262	262
$NCl(CH_3)_2$	N–Cl	177	CNC	108	C···C	230	240
	N–C	142	CINC	107	Cl···C	257	262

Table 17
Bond lengths and bond angles in OX₂ molecules

	OX (pm)	XOX (°)	X···X (pm)
H ₂ O	95.8	104.5	164
F ₂ O	140.9	103.3	220
Cl ₂ O	170.0	110.9	280
(CH ₃) ₂ O	141.0	111.7	234
(SiH ₃) ₂ O	163.4	144.1	311

The bond angles in N(CH₃)₃ and N(SiH₃)₃ are larger than tetrahedral. There are two reasons for these large angles:

- The small size of the central atom compared to the ligand atoms means that ligand–ligand repulsions are relatively more important than in molecules with larger central atoms such as Be and B.
- The valence shell electrons of nitrogen are not strongly localized into pairs because the electronegativity of nitrogen is larger than that of the ligand and so become less important in determining the geometry.

Thus with decreasing electronegativity and increasing size of the ligand repulsions between the ligands become increasingly important so that the bond angles increase and eventually become larger than tetrahedral with increasing size and decreasing electronegativity of the ligand from NF₃ to N(SiH₃)₃.

Table 16 gives the bond angles and bond lengths in some NX₂YE and NXY₂E molecules. If we take one half of the X···X distances from Table 15 as the value of the ligand radius of these ligands when bonded to nitrogen to obtain the values $r(\text{H}) = 82$ pm, $r(\text{F}) = 107$ pm, $r(\text{C}) = 120$ pm and $r(\text{Cl}) = 142$ pm. We can predict the X···Y interligand distances in these molecules. We see from Table 16 that there is good agreement between the predicted and observed values confirming the validity of the LCP model for these molecules.

Table 18
Bond lengths and bond angles in HOX molecules

	O–H (pm)	O–Y (pm)	HOX (°)	X···Y observed (pm)	X···Y predicted (pm)
HOF	96.4	144.2	97.2	183	186
HOCl	97.0	169.3	103	213	216
HOCH ₃	94.5	142.1	108.5	194	193

Table 17 gives values for the bond lengths and bond angles in some OX₂ molecules. Only H₂O and F₂O have bond angles less than the tetrahedral value while Cl₂O and (CH₃)₂O have bond angles that are slightly larger than tetrahedral and that in (SiH₃)₂O is much larger. Again we see that the bond angle increases with increasing size and decreasing electronegativity of the ligand. In the extreme case of a very weakly electronegative ligand such as Li the Li₂O molecule is predominately ionic and to a good approximation can be regarded as (Li⁺)₂O²⁻. In such an ionic molecule there is almost no localization of the valence shell electrons of oxygen into lone pair or bonding pairs. Consequently ligand–ligand interactions dominate the geometry so that the molecule Li₂O is linear.

Table 18 gives bond angles and bond lengths for some HOX molecules. If we assume that the ligand radii can be calculated from the interligand distances in Table 17 we can predict the interligand distances in these molecules and again we see that the agreement is good again confirming the validity of the LCP model. It can at first sight seem surprising that the replacement of a hydrogen in H₂O by a larger ligand, such as F or Cl, leads to a decrease in the bond angle but it must be remembered that the O–F and O–Cl bond lengths are much longer than the O–H bond length.

4.4. Sterically inactive and weakly active lone pairs

The SeCl₆²⁻ ion and several related ions with central atoms of relatively low electronegativity compared to that of the ligands have a regular octahedral geometry [23] which is not in accord with the prediction of the VSEPR model for an AX₆E molecule [24]. So these molecules are often cited as exceptions to the model and are said to have a stereochemically inert lone pair. The LCP model allows us to understand why the nonbonding electrons do not affect the geometry of this and related molecules.

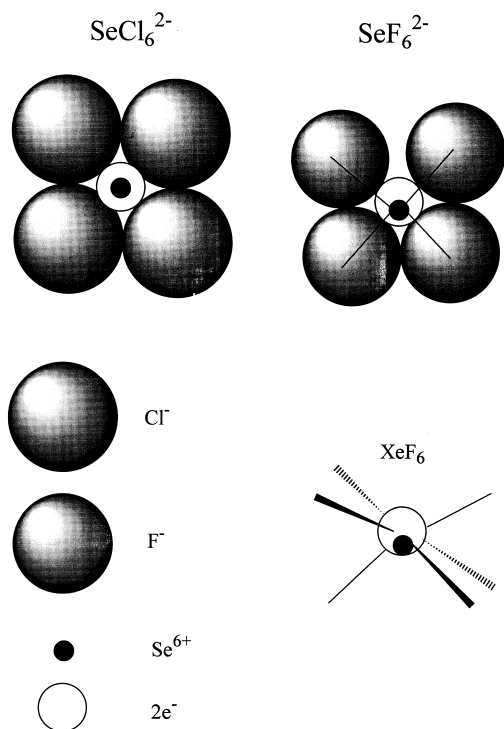


Fig. 5. (a) Representation of close-packing of four Cl^- -like ligands around a central Se^{4+} "core" consisting of the Se^{6+} core and two nonbonding electrons. (b) Representation of the packing of four F^- -like ligands around a slightly distorted Se^{4+} "core" showing the slight protrusion of the two nonbonding electrons into the valence shell causing a small distortion into the valence shell and hence a small distortion from octahedral geometry. (c) Diagram of the distortion of the XeF_6 molecule from octahedral to C_{3v} symmetry by an unsymmetrical Xe^{6+} core.

The relative sizes of the central atom and the ligands allows a maximum coordination number of only four for the Period 2 elements, while for the Period 3 and 4 elements it is six, and it can be even higher for the elements in the later periods. Given that the maximum coordination number for a Period 3 or 4 element is six and that a lone pair behaves like a pseudo ligand, then if there is one lone pair there can be a maximum of only five ligands. These ligands will have a square-pyramidal geometry with the lone pair occupying the sixth position and completing an octahedral AX_5E arrangement, giving an overall square-pyramidal geometry as in SeF_5^- , BrF_5 , and XeF_5^+ [24]. However, if there are six ligands which are close-packed around the central atom there is no

space for a lone pair so that the nonbonding electrons remain on the central atom and the molecule has an octahedral geometry. If SeCl_6^{2-} is regarded as a predominately ionic molecule we can think of it as consisting of six chloride ions octahedrally close-packed around an Se_4^{2+} ion which is composed of an Se^{6+} core surrounded by a spherical distribution of two nonbonding electrons. In other words there is no lone pair localized in the valence shell but rather a delocalized pair of electrons surrounding an Se^{6+} ion (Fig. 5). However, these electrons are not without an influence on the geometry as the $\text{Se}-\text{Cl}$ bonds (241 pm) are considerably longer than in SeCl_2 (215.7 pm). That the Cl ligands are close-packed is strongly suggested by the $\text{Cl}\cdots\text{Cl}$ intermolecular distances of 340 pm, giving a ligand radius of 170 pm. This Cl ligand radius is smaller than the fully ionic radius of Cl^- of 181 pm but considerably larger than the ligand radii of Cl on boron and carbon which are 151 and 144 pm, respectively, consistent with the expected considerably higher negative charge on the Cl ligands in SeCl_6^{2-} .

In contrast to SeCl_6^{2-} , the corresponding fluoride ion SeF_6^{2-} has a distorted octahedral C_{3v} geometry with bond lengths of 202 and 185 pm and bond angles of 111, 95 and 85° which can be described as a mono-capped octahedron with the lone pair in the capping position [25]. In this case the lone pair is said to be only weakly stereochemically active because a fully stereochemically active lone pair would be expected to give an AX_6E pentagonal bipyramidal geometry, analogous to that of the geometry of the pentagonal bipyramidal molecule IOF_6 [26] with the lone pair replacing the oxygen in an axial position. The observed small distortion from an octahedral geometry in SeF_6^{2-} is presumably a consequence of fluorine being a smaller ligand than chlorine but not small enough to allow the two nonbonding electrons to become a true localized lone pair—in other words an E^{2-} pseudo ligand. So the two nonbonding electrons remain largely within the central Se atom, which is therefore closer to an Se^{4+} ion than an Se^{6+} ion. But the Se_4^{2+} ion has a shape that is distorted from spherical (Fig. 4) by the interaction of the fluorine ligands with the two nonbonding electrons. So the geometry of the six surrounding ligands is only slightly distorted from octahedral. The SeF_6^{2-} ion is a borderline example between the majority of molecules in

which lone pairs are fully active and the less common cases such as SeCl_6^{2-} or SeBr_6^{2-} with coordination numbers of six or higher in which the lone pair is stereochemically inactive. Another similar example is provided by the isoelectronic XeF_6 molecule which also has a distorted octahedral C_{3v} geometry (Fig. 5) [27]. If we start from an ionic model we can think of the lone pairs in most molecules as being formed by the interaction of the negative ligands with the nonbonding electrons in the positive central ion which squeezes them out into the valence shell where there is space to accommodate them.

5. Conclusions and summary

We have further extended our recent work in which we showed that the ligand close packing (LCP) model which we developed from observations of constant interligand distances in BeX_n , BX_n and CX_n molecules. This model is an extension of Bartell's similar 1960 suggestion for some CX_n molecules. In particular we have:

1. Further extended the range of ligands to include OX , NX_2 , CH_3 , and Cl .
2. Extended the model to NX_3E and OX_2E_2 molecules, showing that lone pairs behave like pseudo ligands with a size that varies to fill the space available.
3. Shown how the model can be used, for example, to better understand the bond lengths and bond angles in the molecules BF_3 and OCF_3^- .
4. Shown why lone pairs sometimes appear to be stereochemically inactive or only weakly active.
5. Presented a table of ligand radii for C, O, N, H, F, P, S and Cl bonded to Be, B, C, N, O, Si, P and S some of which are preliminary values based on partly unpublished work which will be discussed in forthcoming articles.

We have fully demonstrated that the LCP model in conjunction with the VSEPR model is extremely useful for the understanding of molecular geometry. This model can be expected to have many useful

applications in the future and it will be of interest to extend it in more detail to molecules of Period 3 and beyond.

References

- [1] L.S. Bartell, R.A. Bonham, *J. Chem. Phys.* 32 (1960) 824.
- [2] T. Fukuyama, M. Sugié, I. Tokue, K. Kuchitsu, *Acta Cryst.* A28 (1972) S18.
- [3] L.S. Bartell, *J. Chem. Phys.* 32 (1960) 827.
- [4] L.S. Bartell, K. Kuchitsu, *J. Chem. Phys.* 37 (1962) 691.
- [5] E.J. Jacob, H.B. Thompson, L.S. Bartell, *J. Chem. Phys.* 47 (1967) 3736.
- [6] L.S. Bartell, *J. Chem. Educ.* 45 (1968) 754.
- [7] L.S. Bartell, *Croatica. Chem. Acta* 57 (1984) 927.
- [8] L.S. Bartell, Y.M. Barshad, *J. Am. Chem. Soc.* 106 (1984) 7700.
- [9] I. Hargittai, *The Structure of Volatile Sulfur Compounds*, Reidel, Dordrecht, Boston, Lancaster, 1985.
- [10] See for example M. Hargittai, I. Hargittai, *J. Mol. Struct.* 15 (1973) 399.
- [11] M. Hargittai, I. Hargittai, *J. Mol. Struct.* 20 (1974) 283.
- [12] C. Glidewell, *Inorg. Chimica Acta* 12 (1975) 219.
- [13] C. Glidewell, *Inorg. Chimica Acta* 20 (1976) 113.
- [14] R.J. Gillespie, S.A. Johnson, *Inorg. Chem.* 36 (1997) 3031.
- [15] N.C. Baird, *Inorg. Chem.* 28 (1989) 1224.
- [16] E.A. Robinson, S.A. Johnson, T.-H. Tang, R.J. Gillespie, *Inorg. Chem.* 36 (1997) 3022.
- [17] R.J. Gillespie, I. Bytheway, E.A. Robinson, *Inorg. Chem.* 37 (1998) 2811.
- [18] R.J. Gillespie, E.A. Robinson, *Adv. Mol. Struct. Res.* 4 (1998) 1.
- [19] R.F.W. Bader, *Atoms in Molecules*, Clarendon Press, Oxford, 1880.
- [20] R.J. Gillespie, G.L. Heard, E.A. Robinson, unpublished work.
- [21] R.J. Gillespie, E.A. Robinson, G.L. Heard, *Inorg. Chem.* 37 (1998).
- [22] K.B. Wiberg, *J. Am. Chem. Soc.* 112 (1990) 3379.
- [23] R.J. Gillespie, E.A. Robinson, *Angew. Chem. Int. Ed. Engl.* 35 (1996) 495.
- [24] R.J. Gillespie, I. Hargittai, *The VSEPR Model of Molecular Geometry*, Allyn and Bacon, Boston, 1991.
- [25] A.R. Mahjoub, X. Zhang, K. Seppelt, *Chem. Eur. J.* 1 (1995) 261.
- [26] K.O. Christe, D.A. Dixon, A.R. Mahjoub, H.P.A. Mercier, J.C.P. Saunders, G.J. Schrobilgen, W.W. Wilson, *J. Am. Chem. Soc.* 115 (1993) 2696.
- [27] R.M. Gavin, L.S. Bartell, *J. Chem. Phys.* 48 (1968) 2466.